


Received 18 June 2024, accepted 11 July 2024, date of publication 16 July 2024, date of current version 24 July 2024.

Digital Object Identifier 10.1109/ACCESS.2024.3429399

RESEARCH ARTICLE

Optimal Scheduling of Combined Heat and Power Systems Integrating Hydropower-Wind-Photovoltaic-Thermal-Battery Considering Carbon Trading

SHENGGANG ZHU¹, ENZHONG WANG², SHAOZU HAN¹, AND HUICHAO JI¹

¹CHN Energy Technology & Environment Group Co., Ltd., Beijing 100039, China

²Guoneng Qinghai Yellow River Maerdang Hydropower Development Co., Ltd., Qinghai 814000, China

³School of Automation Engineering, Northeast Electric Power University, Jilin City 132012, China

Corresponding author: Huichao Ji (huichaoji@neepu.edu.cn)

This work was supported in part by the Research and Engineering Demonstration of a Fully Clean Energy Safe, Autonomous, and Controllable Smart Management and Control System at the 10-GW Level under Grant CSIEKJ220700539; and in part by the Ph.D. Scientific Research Startup Foundation of Northeast Electric Power University under Grant BSJXM-2022209.

ABSTRACT During the winter heating period, the accommodation of wind and photovoltaic (PV) power is limited due to the prioritized scheduling of combined heat and power (CHP) systems to meet the heat load demand of users, which indirectly increases carbon emissions (CE). Due to the robust peak shaving and energy storage capabilities of pumped storage hydropower (PSH), PSH and tiered carbon trading can be employed to address these issues. However, there are scarce reports on research exploring the integration of PSH and carbon trading into CHP systems. To fill the technology gap, we propose a low-carbon optimal scheduling method that integrates hydropower-wind-PV-thermal-battery (HWPTB) with CHP. The scheduling model for coordinated multi-energy complementarity of HWPTB is developed to address the electric and heat demand of users. The proposed work is validated by numerical simulation, compared with the traditional optimal scheduling method without considering PSH and carbon trading, the wind and PV power curtailment rates are reduced by 7.17% and 6.77%, respectively, and the operation cost is also reduced by 43.6%, and the CE cost is -4163.3 (\$). The results show that the PSH can shave the peak of the electric load and alleviate the reduction of renewable energy accommodation, with no increase in operation cost and profit by tiered carbon trading.

INDEX TERMS Optimal scheduling, combined heat and power systems, pumped storage hydropower, tiered carbon trading, hydropower-wind-PV-thermal-battery.

NOMENCLATURE

ABBREVIATIONS


CE	Carbon emission.
CHP	Combined heat and power.
DHN	District heating network.
EL	Electric load.
HL	Heat load.
HP	Heat power.
HST	Heat storage tank.
HWPTB	Hydropower-wind-photovoltaic-thermal-battery.

PV	Photovoltaic.
PVPC	Photovoltaic power curtailment.
PSH	Pumped storage hydropower.
TOU	Time-of-use.
TPP	Thermal power plant.
WPC	Wind power curtailment.
WPP	Wind power plant.

I. INTRODUCTION

A. MOTIVATION

As global climate change intensifies, the need to reduce carbon emissions (CE) and enhance the utilization rate of

The associate editor coordinating the review of this manuscript and approving it for publication was Ehab Elsayed Elattar .

renewable energy has become urgent [1], [2], [3]. However, the accommodation of wind and photovoltaic (PV) power is being limited by the constraints of grid access capacity, system stability, and the prioritized scheduling of combined heat and power (CHP) systems, especially during the heating period in winter, when the demand for heat load limits the power output [4], [5], [6]. This not only reduces the utilization of renewable energy, but also increases CE, which has negative environmental impacts. To tackle this challenge, considering the abundant water resources in Northwest China, hydropower can be utilized due to its high flexibility and minimal environmental impact. However, existing research rarely reports on optimal scheduling methods that combine CHP and hydropower. Therefore, to fill this knowledge gap, the motivation of this paper is to effectively utilize hydropower in combined electricity and heat systems (CEHS), thus enhancing the accommodation of clean energy and reducing CE.

B. LITERATURE REVIEW

With regard to improve renewable energy accommodation for CHP, the problem is discussed in the existing studies from multiple perspectives, which can be categorized into the following aspects *a-c*):

a) Due to the electric-thermal coupling characteristics of CHP, the heat load limits the heat power (HP) output [7]. Thus, the space for clean energy accommodation is reduced. Therefore, scholars improve the clean energy accommodation by reducing the CHP's output heat power. Chen et al. [8] propose the utilization of heat storage tank (HST) in CHP systems, which can store excess heat during periods of low electricity demand or oversupply of heat sources, and release the stored heat to meet heating demand during peak electricity demand or insufficient heat supply. The WPC rate is primarily reduced by introducing HST when wind power and CHP are integrated. Du et al. [9] consider the seasonal district heating network (DHN) reconfiguration in the CHP system, and the simulation results show that the DHN reconfiguration can enhance the wind power accommodation. Lin et al. [10] propose a joint commitment method of CHP and heat exchange stations, the numerical simulations demonstrated that the total WPC is reduced and the economic benefit gained by introducing heat exchange stations. Liu et al. [11] present an optimal economic scheduling model of CHP to minimize the total operation cost and WPC by using electric boilers. The result shows that WPC can be reduce by using the electric boilers.

The above-mentioned studies have conducted joint optimal scheduling of CHP with HST, DHN, heat exchange stations, and electric boilers, respectively, aiming to improve the flexibility of CHP regulation by regulating HP, thereby enhancing the accommodation of clean energy. However, heat-related equipment exhibits significant inertia, limiting its ability to respond effectively to rapidly fluctuating loads and variable renewable energy outputs. Therefore, some scholars propose using electric energy storage technology,

which can improve the accommodation of clean energy due to its rapid response capability.

b) The application of batteries in improving the flexibility of CHP regulation. Elkadeem and Abido [12] propose a model for optimal scheduling and operation of an integrated CHP with battery, the results show that increasing the utilization rate of CHP and batteries can fully utilize PV power. Sarlak et al. [13] present a hybrid system of CHP-boiler-battery, the proposed scheme succeeded in improving the flexibility of CHP. Shi et al. [14] explore a pattern of CHP-boiler-PV-battery to supply the electricity demand, and the boiler is used to supply the heat demand. The results of studies on electric energy storage can improve the accommodation of renewable energy by storing electricity. However, the accommodation of renewable energy by batteries is related to capacity, which increases the operation cost of the system.

In the optimal scheduling of CHP, a variety of methods to improve the flexibility of CHP regulation and increase the accommodation of clean energy have been reviewed from the aspects of electric and heat power. However, these aspects are constrained by thermal inertia and operational costs. Therefore, considering the abundant water resources in Northwest China, the pumped storage hydropower (PSH) can be used in the optimal scheduling of CHP.

c) The working characteristics of PSH are similar to those of the aforementioned HST and battery. During valley periods, they pump water from the lower reservoir to the upper one. Then, during peak hours, the potential energy of the water in the upper reservoir is converted back into electrical energy. Naval et al. [15] present an optimal hourly management model of grid-connected PV and wind power plants (WPP) integrated with PSH. The simulation results show that compared to a system without storage, the combination of renewable energy and PSH reduces energy dependence and decreases energy costs by 27%. Guo et al. [16] propose a PV-wind-hydro hybrid power system with PSH and thermal energy storage, the simulation results indicate that the proposed system has better economy and reliability performance. Ren et al. [17] explore a method to solve the problem of curtailment in wind and PV generation systems and establish a combined PSH-wind-PV-hydrogen production system. Li et al. [18] combine wind-PV and PSH, and establish the cooperative operation model of joint participation in the electric energy market and auxiliary service market. The overall benefit of the multi-energy complementary system is enhanced by the output complementarity of the hydropower, PV, and wind power units, as well as the flexibility support of the PSH units. Amoussou et al. [19] develop a numerical model that explains how an integrated energy framework consisting of PV, wind turbines, and PSH system integrated with the electric utility operates in parallel. The existing research applies the PSH to various power system scenarios where the peak can be shaved. However, the scarcity of studies integrating CHP and PSH, and the lack of studies pointing to a correlation between

TABLE 1. Comparison between this work and existing works.

Units/Ref.	[6]	[7]	[8]	[9]	[10]	[11]	[12]	[13]	[14]	[15]	[16]	[17]	[18]	[19]	[20]	[21]	[22]	[23]	[24]	This work
HP	✓	✓	✓	✓	✓	✓	✓	✓	✓	✗	✓	✗	✗	✗	✓	✓	✗	✓	✓	✓
CHP	✓	✓	✓	✓	✓	✓	✓	✓	✓	✗	✓	✗	✗	✗	✓	✓	✗	✓	✓	✓
TPP	✓	✓	✓	✓	✓	✓	✓	✗	✗	✗	✗	✗	✗	✓	✓	✓	✓	✗	✗	✓
PSH	✗	✗	✗	✗	✗	✗	✗	✗	✗	✓	✓	✓	✓	✓	✗	✗	✓	✗	✗	✓
WPP	✗	✗	✓	✓	✓	✓	✓	✓	✓	✓	✓	✓	✓	✓	✓	✓	✓	✓	✗	✓
PV	✗	✗	✗	✗	✗	✗	✓	✓	✓	✓	✓	✓	✓	✓	✗	✓	✓	✓	✓	✓
Battery	✗	✗	✗	✗	✗	✗	✓	✓	✓	✗	✗	✓	✗	✗	✗	✗	✗	✓	✓	✓
Boiler	✗	✗	✗	✓	✗	✓	✓	✓	✓	✗	✓	✗	✗	✗	✗	✓	✗	✓	✓	✓
CE	✗	✗	✗	✗	✗	✗	✗	✗	✗	✗	✗	✗	✗	✗	✗	✗	✓	✓	✓	✓

the two, motivates us to address the technological gap in this area.

Traditional CHP is still based on coal combustion, the consumption of coal for thermal power generation causes severe air pollution in the Beijing-Tianjin-Hebei region [20]. Scholars suggest reducing the feed-in tariff for wind power during the “14th Five-Year plan.” Therefore, considering carbon trading in a new power system dominated by renewable energy is a current research hotspot. Zou et al. [21] propose a dynamic economic emission scheduling that integrates CHP, wind power, and PV. The pollutant emission is considered in the model, and the generation costs and pollutant emissions are reduced by the proposed method. Wang et al. [22] explore renewable energy options for sustainable economic growth without CE: An in-depth comparative analysis exploring the economic and environmental impacts of turbines, PV, and hydropower, the research results reveal that wind, PV, and hydro energy lower CE. Xiang et al. [23] propose a hierarchical distributed dispatch model of multiple energy systems considering carbon trading, the different CE sources include CHP, gas boilers, and power to gas devices. Cao et al. [24] address the issue of carbon management and resource allocation in an intelligent community with CHP, PV, battery, and boiler. The results of the above studies show that considering pollutant emissions can improve new energy accommodation. Based on this study, this paper incorporates stepped carbon trading into a system that integrates CHP and PSH, in order to reveal its impact on system operation costs and new energy accommodation.

C. CONTRIBUTIONS AND PAPER ORGANIZATIONS

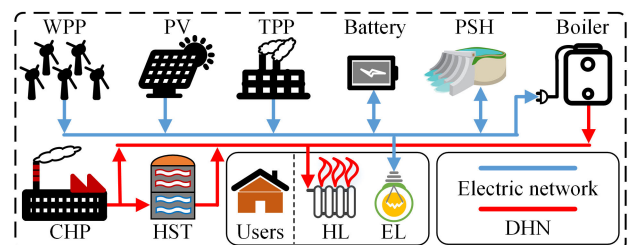
Due to the priority schedule of CHP, the accommodation of renewable energy is reduced to meet the demand for heat load, resulting in increased CE. PSH can alleviate the issue of CHP’s electric power output through the mutual conversion of electrical energy and potential energy. However, the PSH and tiered carbon trading are not considered in the CHP systems to solve the above concerns. To fill the technology gap, this paper proposes a low-carbon optimal scheduling method that integrates hydropower-wind-PV-thermal-battery (HWPTB) with CHP. The comparison of this work with other similar published works is shown in Table 1. The contributions of this paper are presented to address the above challenges and can be outlined as follows:

- To the best of the author’s knowledge, it is the first time that the optimal scheduling of CHP systems integrating hydropower-wind-PV-thermal-battery is proposed, and the stepped carbon trading is considered in this combined system;
- An optimal scheduling model for HWPTB with CHP is developed. This model can not only utilize PSH to shave the peak of the electric load (EL) and alleviate the reduction of renewable energy accommodation space caused by the CHP’s heat load (HL) constraints, but also reduce CE and improve the economy of system operation through tiered carbon trading;
- The proposed work is validated by four cases, with WPC rates of 7.39%, 6.63%, 4.74%, and 0.22%, and the photovoltaic power curtailment (PVPC) rates of 7.2%, 6.38%, 4.96%, and 0.43%. Compared with the traditional optimal scheduling method without considering carbon trading and PSH, the WPC and PVPC are reduced by 7.17% and 6.77%, respectively, and the operation cost is also reduced by 43.6%. The CE cost is -4163.3 (\$), which shows no increase in the operation cost and profit by tiered carbon trading.

The rest of this paper is organized as follows: The system structure of CHP integrating HWPTB is described in Section II. Optimal scheduling models of CHP integrating HWPTB and tiered carbon trading are illustrated in Section III. The numerical simulations of four cases are validated in Section IV. Section V is the conclusion.

II. SYSTEM STRUCTURE OF CHP INTEGRATING HWPTB

The structure of CHP integrating HWPTB is illustrated in Figure 1.

**FIGURE 1.** The system structure of CHP integrating HWPTB.

The system structure includes WPP, PV, thermal power plant (TPP), battery, PSH, boiler, CHP, HST, EL, and HL. The arrows in Figure 1 indicate the flow direction of electric and thermal energy. EL is powered by WPP, PV, TPP, Battery, PSH and CHP. The electric energy during the valley period is stored in the Battery. PSH uses the excess electric energy to pump water from the downstream reservoir to the upstream reservoir, then releases it during the peak period. CHP, HST, and Boiler supply HL and the HST is used to store the excess thermal energy generated by CHP, and the stored thermal energy is released when HST demand increases. The boiler consumes the electric energy to generate thermal energy, which is output to the DHN to assist with CHP regulation.

III. OPTIMAL SCHEDULING MODELS OF CHP INTEGRATING HWPTB AND TIERED CARBON TRADING

A. OBJECTIVE FUNCTION

The operating costs of the CHP system integrating HWPTB include the fuel coal costs of TPP and CHP units, the costs of wind and PV power curtailment, the operating cost of the boiler based on TOU prices, the operating and maintenance costs of thermal and electric power storage in HST and battery, the pumping and generation costs of PSH, and the costs of tiered carbon trading. The objective function of the system is to minimize the operating costs of the above units, the objective function C is expressed as (1).

$$\begin{aligned} \text{Min}C = & \sum_{t \in \mathcal{T}} \sum_{f \in \mathcal{I}^{\text{TPP}}} C(P_{f,t}) + \sum_{t \in \mathcal{T}} \sum_{b \in \mathcal{I}^{\text{CHP}}} C(P_{b,t}, H_{b,t}) \\ & + \sum_{t \in \mathcal{T}} \sum_{k \in \mathcal{I}^{\text{HST}}} C(H_{k,t}^+, H_{k,t}^-) + \sum_{t \in \mathcal{T}} \sum_{g \in \mathcal{I}^{\text{WPP}}} C(P_{g,t}) \\ & + \sum_{t \in \mathcal{T}} \sum_{e \in \mathcal{I}^{\text{Battery}}} C(P_{e,t}^+, P_{e,t}^-) + \sum_{t \in \mathcal{T}} \sum_{r \in \mathcal{I}^{\text{PV}}} C(P_{r,t}) \\ & + \sum_{t \in \mathcal{T}} \sum_{s \in \mathcal{I}^{\text{PSH}}} C(P_{s,t}^+, P_{s,t}^-) + \sum_{t \in \mathcal{T}} \sum_{z \in \mathcal{I}^{\text{Boiler}}} C(P_{z,t}) \\ & + C^{\text{CE}}(E_q - E_d) \end{aligned} \quad (1)$$

where \mathcal{I}^{TPP} , \mathcal{I}^{CHP} , \mathcal{I}^{WPP} , \mathcal{I}^{PV} , $\mathcal{I}^{\text{Boiler}}$, \mathcal{I}^{HST} , $\mathcal{I}^{\text{Battery}}$, and \mathcal{I}^{PSH} are the set of indices of TPP, CHP, WPP, PV, Boiler, HST, Battery, and PSH, respectively, the $C(P_{f,t})$, $C(P_{b,t}, H_{b,t})$, $C(P_{g,t})$, $C(P_{r,t})$, $C(P_{z,t})$, $C(H_{k,t}^+, H_{k,t}^-)$, $C(P_{e,t}^+, P_{e,t}^-)$, $C(P_{s,t}^+, P_{s,t}^-)$, and $C^{\text{CE}}(E_q - E_d)$ are the operating costs function of the TPP, CHP, WPP, PV, Boiler, HST, Battery, PSH, and CE, respectively, T is the set of indices of scheduling periods, $t \in \{1, 2, \dots, |\mathcal{T}|\}$, $P_{f,t}$ is the scheduled electric power of the f th TPP at time t , $P_{b,t}$ and $H_{b,t}$ are the scheduled electric and thermal power of the b th CHP at time t , respectively, $P_{g,t}$ is the scheduled electric power of the g th WPP at time t , $P_{r,t}$ is the scheduled electric power of the r th PV at time t , $P_{z,t}$ is the scheduled electric power of the z th boiler at time t , $H_{k,t}^+$ and $H_{k,t}^-$ are the charging and discharging thermal power of the k th HST at time t , $P_{e,t}^+$ and $P_{e,t}^-$ are the charging and discharging electric power of the e th battery at time t , $P_{s,t}^+$

and $P_{s,t}^-$ are the hydropower and pumping power of the s th PSH at time t , E_q is the total CE quota, E_d is the total CE of the system during a scheduling period.

B. OPERATION COSTS AND CONSTRAINTS

1) TPP

The electric power required by the grid is supplied by TPP, and its operating cost is coal consumption. The calculation of the operating cost is shown in (2).

$$C(P_{f,t}) = \xi_{f,0}(P_{f,t})^2 + \xi_{f,1}P_{f,t} + \xi_{f,2} \quad \forall f \in \mathcal{I}^{\text{TPP}}, t \in \mathcal{T} \quad (2)$$

where the $\xi_{f,0}$, $\xi_{f,1}$, and $\xi_{f,2}$ are operating cost coefficients of the f th TPP, $\xi_{f,0}$ represents the slope of coal consumption varying with load, $\xi_{f,1}$ reflects the linear part of coal consumption, $\xi_{f,2}$ is the fixed cost of coal consumption.

The operating constraints of TPP include output electric power and ramp rate limits, the constraints are shown in (3) and (4).

$$P_{f,\min} \leq P_{f,t} \leq P_{f,\max} \quad \forall f \in \mathcal{I}^{\text{TPP}}, t \in \mathcal{T} \quad (3)$$

$$\begin{aligned} R_{f,\text{down}} \times \Delta t \leq P_{f,t} - P_{f,t-1} \leq R_{f,\text{up}} \times \Delta t \\ \forall f \in \mathcal{I}^{\text{TPP}}, t \in \mathcal{T} \end{aligned} \quad (4)$$

where $P_{f,\min}$ and $P_{f,\max}$ are the minimum and maximum output electric power of the f th TPP, $R_{f,\text{down}}$ and $R_{f,\text{up}}$ are the downward and upward ramp rate of the f th TPP, Δt is the scheduling time interval.

2) CHP

The CHP supplies the electric power of grid and thermal power of DHN, the fuel cost of CHP is shown in (5).

$$\begin{aligned} C(P_{b,t}, H_{b,t}) = \xi_{b,0}[P_{b,t} + v_b H_{b,t}]^2 + \xi_{b,1}[P_{b,t} + v_b H_{b,t}] \\ + \xi_{b,2} \quad \forall b \in \mathcal{I}^{\text{CHP}}, t \in \mathcal{T} \end{aligned} \quad (5)$$

where $\xi_{b,0}$, $\xi_{b,1}$, and $\xi_{b,2}$ are operating cost coefficients of the b th CHP, v_b is the reduction of power generation when the b th CHP extracts per unit of heat with a constant air intake.

The operating region of the CHP is typically a polygon, and the boundaries of this polygon are defined by the unit's maximum and minimum electrical power output and thermal power output. These constraints ensure that the unit does not exceed its design capacity and operating range, as shown in (6).

$$\begin{cases} (P_{b,\min} - v_{b,0}H_{b,t}) \leq P_{b,t} \leq (P_{b,\max} - v_{b,2}H_{b,t}) \\ v_{b,1}(H_{b,t} - H_{b,\text{med}}) \leq P_{b,t} \\ 0 \leq H_{b,t} \leq H_{b,\text{max}} \\ R_{b,\text{down}} \times \Delta t \leq P_{b,t} - P_{b,t-1} \leq R_{b,\text{up}} \times \Delta t \\ \forall b \in \mathcal{I}^{\text{CHP}}, t \in \mathcal{T} \end{cases} \quad (6)$$

where $P_{b,\min}$ and $P_{b,\max}$ are the minimum and maximum output electric power of the b th CHP, $v_{b,0}$ and $v_{b,2}$ are the minimum and maximum reduction of electric power of the b th CHP, $v_{b,1}$ is the back-pressure curve slope of the b th

CHP, $H_{b,\text{med}}$ is the thermal power of minimum electric power output of the b th CHP, $H_{b,\text{max}}$ is the maximum thermal power limit of the b th CHP, $R_{b,\text{down}}$ and $R_{b,\text{up}}$ are the downward and upward ramp rate of the b th CHP.

3) HST

The HST is located between the CHP and the DHN, the excess thermal energy can be stored in the HST and released when the electric power of the CHP decreases. The operating cost of HST includes the operation and maintenance, and the investment cost of the rated power and capacity. The operating cost of HST is shown in (7).

$$C(H_{k,t}^+, H_{k,t}^-) = \xi_{k,0}(H_{k,t}^+ + H_{k,t}^-) + [(\xi_{k,1}H_{k,\text{rated}} + \xi_{k,2}S_{k,\text{max}})/T_k] \quad \forall k \in \mathcal{I}^{\text{HST}}, t \in \mathcal{T} \quad (7)$$

where $\xi_{k,0}$, $\xi_{k,1}$, and $\xi_{k,2}$ are the operation and maintenance, rated power and capacity cost coefficients of the k th HST, T_k is the service life of the k th HST.

The thermal power and thermal energy storage capacity constraints of HST are shown in (8) and (9).

$$\begin{cases} S_{k,t} = \beta_k S_{k,t-1} + H_{k,t}^+ - H_{k,t}^- \\ 0 \leq S_{k,t} \leq S_{k,\text{max}} \\ H_{k,t}^+ + S_{k,t-1} \leq S_{k,\text{max}} \\ H_{k,t}^- - S_{k,t-1} \leq 0 \end{cases} \quad \forall k \in \mathcal{I}^{\text{HST}}, t \in \mathcal{T} \quad (8)$$

$$\begin{cases} 0 \leq H_{k,t}^+ \leq H_{k,\text{rated}}\varepsilon_{k,t}^+ \\ 0 \leq H_{k,t}^- \leq H_{k,\text{rated}}\varepsilon_{k,t}^- \\ \varepsilon_{k,t}^+ + \varepsilon_{k,t}^- \leq 1 \\ \varepsilon_{k,t}^+, \varepsilon_{k,t}^- \in \{0, 1\} \end{cases} \quad \forall k \in \mathcal{I}^{\text{HST}}, t \in \mathcal{T} \quad (9)$$

where $S_{k,t}$ is the thermal energy storage capacity of the k th HST at time t , β_k is the efficiency of the k th HST at time t , $S_{k,\text{max}}$ is the maximum storage capacity of the k th HST at time t , $H_{k,\text{rated}}$ is the rated power of the k th HST at time t , $\varepsilon_{k,t}^+$ and $\varepsilon_{k,t}^-$ is the binary variable associated with charging and discharging of the k th HST at time t , $\varepsilon_{k,t}^+ + \varepsilon_{k,t}^- \leq 1$ denotes that the k th HST cannot charging and discharging simultaneously at time t .

4) WPP

The operation cost of WPP is the penalty of WPC, as shown in (10).

$$C(P_{g,t}) = \xi_{g,0}(\bar{P}_{g,t} - P_{g,t}) \quad \forall g \in \mathcal{I}^{\text{WPP}}, t \in \mathcal{T} \quad (10)$$

where $\bar{P}_{g,t}$ is the predicted wind power of the g th WPP at time t .

The upper limit of WPP output power is shown in (11).

$$0 \leq P_{g,t} \leq \bar{P}_{g,t} \quad \forall g \in \mathcal{I}^{\text{WPP}}, t \in \mathcal{T} \quad (11)$$

5) PV

The operation cost of PV is the penalty of PVPC, as shown in (12).

$$C(P_{r,t}) = \xi_{r,0}(\bar{P}_{r,t} - P_{r,t}) \quad \forall r \in \mathcal{I}^{\text{PV}}, t \in \mathcal{T} \quad (12)$$

where $\bar{P}_{r,t}$ is the predicted photovoltaic power of the r th PV at time t .

The upper limit of PV output power is shown in (13).

$$0 \leq P_{r,t} \leq \bar{P}_{r,t} \quad \forall r \in \mathcal{I}^{\text{PV}}, t \in \mathcal{T} \quad (13)$$

6) BATTERY

The excess electrical energy output from TPP, CHP, WPP, PV, and PSH is stored by the battery and released during peak load periods. The power fluctuation can be mitigated by the battery storage and release of electrical energy. The operating cost of the battery includes the operation and maintenance, and the investment cost of the rated power and capacity. The operating cost of the battery is shown in (14).

$$C(P_{q,t}^+, P_{q,t}^-) = \xi_{q,0}(P_{q,t}^+ + P_{q,t}^-) + [(\xi_{q,1}P_{q,\text{rated}} + \xi_{q,2}S_{q,\text{max}})/T_q] \quad \forall q \in \mathcal{I}^{\text{Battery}}, t \in \mathcal{T} \quad (14)$$

where $\xi_{q,0}$, $\xi_{q,1}$, and $\xi_{q,2}$ are the operation and maintenance, rated power and capacity cost coefficients of the q th battery, T_q is the service life of the q th battery.

The electric power and electric energy storage capacity constraints of the battery are shown in (15) and (16).

$$\begin{cases} S_{q,t} = \beta_q S_{q,t-1} + P_{q,t}^+ - P_{q,t}^- \\ 0 \leq S_{q,t} \leq S_{q,\text{max}} \\ P_{q,t}^+ + S_{q,t-1} \leq S_{q,\text{max}} \\ P_{q,t}^- - S_{q,t-1} \leq 0 \end{cases} \quad \forall q \in \mathcal{I}^{\text{Battery}}, t \in \mathcal{T} \quad (15)$$

$$\begin{cases} 0 \leq P_{q,t}^+ \leq P_{q,\text{rated}}\varepsilon_{q,t}^+ \\ 0 \leq P_{q,t}^- \leq P_{q,\text{rated}}\varepsilon_{q,t}^- \\ \varepsilon_{q,t}^+ + \varepsilon_{q,t}^- \leq 1 \\ \varepsilon_{q,t}^+, \varepsilon_{q,t}^- \in \{0, 1\} \end{cases} \quad \forall q \in \mathcal{I}^{\text{Battery}}, t \in \mathcal{T} \quad (16)$$

where $S_{q,t}$ is the electric energy storage capacity of the q th battery at time t , β_q is the efficiency of the q th battery at time t , $S_{q,\text{max}}$ is the maximum storage capacity of the q th battery at time t , $H_{q,\text{rated}}$ is the rated power of the q th battery at time t , $\varepsilon_{q,t}^+$ and $\varepsilon_{q,t}^-$ is the binary variable associated with charging and discharging of the q th battery at time t , $\varepsilon_{q,t}^+ + \varepsilon_{q,t}^- \leq 1$ denotes that the q th battery cannot charge and discharge simultaneously at time t .

7) CE

The tiered carbon trading mechanism is an emission reduction mechanism that treats CE as a freely traded commodity. The allocation of CE allowances is based on a baseline approach, where CE quotas are proportional to the output of thermal power units. System CE quotas are calculated shown in (17).

$$E_q = \epsilon_f \sum_{t \in \mathcal{T}} \sum_{f \in \mathcal{I}^{\text{TPP}}} P_{f,t} + \epsilon_b \sum_{t \in \mathcal{T}} \sum_{b \in \mathcal{I}^{\text{CHP}}} P_{b,t} + \epsilon_g \sum_{t \in \mathcal{T}} \sum_{g \in \mathcal{I}^{\text{WPP}}} P_{g,t} + \epsilon_r \sum_{t \in \mathcal{T}} \sum_{r \in \mathcal{I}^{\text{PV}}} P_{r,t}$$

$$\forall f \in \mathcal{I}^{\text{TPP}}, b \in \mathcal{I}^{\text{CHP}}, g \in \mathcal{I}^{\text{WPP}}, r \in \mathcal{I}^{\text{PV}}, t \in \mathcal{T} \quad (17)$$

where ϵ_f , ϵ_b , ϵ_g , and ϵ_r are the emission allowance per unit of electricity of f th TPP, b th CHP, g th WPP, and r th PV, respectively.

Wind and photovoltaic power are renewable energy and do not generate CE, which are generated by conventional TPP and CHP units, and the calculation formula is shown in (18).

$$E_d = \sum_{t \in \mathcal{T}} \sum_{f \in \mathcal{I}^{\text{TPP}}} \beta_f P_{f,t} + \sum_{t \in \mathcal{T}} \sum_{b \in \mathcal{I}^{\text{CHP}}} \beta_b P_{b,t} \quad (18)$$

$$\forall f \in \mathcal{I}^{\text{TPP}}, b \in \mathcal{I}^{\text{CHP}}, t \in \mathcal{T}$$

where β_f and β_b are CE intensity of the f th TPP and b th CHP, respectively.

According to the CE and carbon trading price, To regulate and reduce the CE of the system, a tiered carbon trading cost model is adopted for the combined system, i.e., the cost range of carbon trading is determined by the tiered interval where the CE is located. The E_q of the system is less than the CE quota E_d . $C^{\text{CE}}(\cdot)$ is a negative value, the excess CE quota can be traded in the carbon trading market at the initial CE price to obtain carbon revenue. Conversely, $C^{\text{CE}}(\cdot)$ is a positive value, the actual CE E_q of the system is larger than the quota E_d , penalty is imposed on CE more than the quota. The tiered carbon trading cost model is shown in (19).

$$\begin{cases} C^{\text{CE}} = \omega (E_d - E_q), \\ \text{if } E_d \leq E_q + \kappa \\ C^{\text{CE}} = \omega \kappa + (1 + \varphi) \omega (E_d - E_q - \kappa), \\ \text{if } E_q + \kappa < E_d \leq E_q + 2\kappa \\ C^{\text{CE}} = (2 + \varphi) \omega \kappa + (1 + 2\varphi) \omega (E_d - E_q - 2\kappa), \\ \text{if } E_d > E_q + 2\kappa \end{cases} \quad (19)$$

where ω is the carbon trading price, κ is the interval of CE, φ is the increase in the carbon trading price for each additional tier of CE.

8) BOILER

The electric boiler is a device that converts electrical energy into thermal energy. The boiler can be used to replace CHP for heating when there is an excess of renewable energy and a high demand of HL.

$$C(P_{z,t}) = \xi_{z,t} * P_{z,t} \quad \forall z \in \mathcal{I}^{\text{Boiler}}, t \in \mathcal{T} \quad (20)$$

where $\xi_{z,t}$ is the TOU prices of the z th boiler at time t .

The maximum limit of the boiler is shown in (21).

$$0 \leq P_{z,t} \leq P_{z,\max} \quad \forall z \in \mathcal{I}^{\text{Boiler}}, t \in \mathcal{T} \quad (21)$$

where $P_{z,\max}$ is the maximum power of the z th boiler.

9) PSH

PSH is a renewable energy, and the PSH consumes a certain amount of electricity during the energy storage process. The generation of electricity needs to consider operation and maintenance costs. The operating cost of PSH is shown in (22).

$$C(P_{s,t}^+, P_{s,t}^-) = \xi_{s,0} P_{s,t}^+ + \xi_{s,1} P_{s,t}^- \quad \forall s \in \mathcal{I}^{\text{PSH}}, t \in \mathcal{T} \quad (22)$$

where $\xi_{s,0}$ is the cost of the s th PSH power generation and maintenance, $\xi_{s,1}$ is the cost of the s th PSH.

The constraints of PSH include pumping power, reservoir capacity, power generation, and pumped storage operating condition, the limits are shown in (23)-(27).

$$P_{s,\min}^+ \leq P_{s,t}^+ \leq \min(P_{s,\max}^+, \beta_{s,0} E_{s,t} / \Delta t) \quad \forall s \in \mathcal{I}^{\text{PSH}}, t \in \mathcal{T} \quad (23)$$

$$P_{s,\min}^- \leq P_{s,t}^- \leq P_{s,\max}^- \quad \forall s \in \mathcal{I}^{\text{PSH}}, t \in \mathcal{T} \quad (24)$$

$$E_{s,t} = E_{s,t-1} + \Delta t * (\beta_{s,1} P_{s,t}^- - P_{s,t}^+ / \beta_{s,0}) \quad \forall s \in \mathcal{I}^{\text{PSH}}, t \in \mathcal{T} \quad (25)$$

$$\begin{cases} E_{s,\min} \leq E_{s,t} \leq E_{s,\max} \\ E_{s,t} = E_{s,\text{ini}} \end{cases} \quad \forall s \in \mathcal{I}^{\text{PSH}}, t \in \mathcal{T} \quad (26)$$

$$P_{s,t}^+ * P_{s,t}^- = 0 \quad \forall s \in \mathcal{I}^{\text{PSH}}, t \in \mathcal{T} \quad (27)$$

where $P_{s,\min}^+$ and $P_{s,\max}^+$ are the minimum and maximum output hydropower of the s th PSH, $\beta_{s,0}$ is the hydropower efficiency of the s PSH, $E_{s,t}$ is the reservoir storage energy of the s th PSH at time t , $P_{s,\min}^-$ and $P_{s,\max}^-$ are the minimum and maximum pumping power of the s th PSH, $\beta_{s,1}$ is the pumping efficiency of the s PSH, $E_{s,\min}$ and $E_{s,\max}$ are the minimum and maximum reservoir storage energy of the s th PSH, $E_{s,\text{ini}}$ is the initial reservoir storage energy of the s th PSH, $P_{s,t}^+ * P_{s,t}^- = 0$ denotes that the s th PSH cannot generate electricity and pump water simultaneously at time t .

C. ELECTRIC AND THERMAL NETWORK CONSTRAINTS

1) ELECTRIC NETWORK BALANCE CONSTRAINT

$$\begin{aligned} & \sum_{f \in \mathcal{I}^{\text{TPP}}} P_{f,t} + \sum_{b \in \mathcal{I}^{\text{CHP}}} P_{b,t} + \sum_{g \in \mathcal{I}^{\text{WPP}}} P_{g,t} + \sum_{r \in \mathcal{I}^{\text{PV}}} P_{r,t} \\ & + \sum_{q \in \mathcal{I}^{\text{Battery}}} P_{q,t}^- + \sum_{s \in \mathcal{I}^{\text{PSH}}} P_{s,t}^+ = P_t^L + \sum_{q \in \mathcal{I}^{\text{Battery}}} P_{q,t}^+ \\ & + \sum_{s \in \mathcal{I}^{\text{PSH}}} P_{s,t}^- + \sum_{z \in \mathcal{I}^{\text{Boiler}}} P_{z,t} \quad \forall t \in \mathcal{T} \end{aligned} \quad (28)$$

where P_t^L is the EL at time t .

2) TRANSMISSION CAPACITY CONSTRAINT

The DC power flow model is adopted for modeling the power system network structure, and the constraints of the power flow and power balance of each branch are shown in (29).

$$P_{(i,j),t} = B_{(i,j)} (\theta_{i,t} - \theta_{j,t}) \quad \forall (i,j) \in \mathcal{I}^{\text{LINE}}, t \in \mathcal{T}, \theta_{\text{ref},t} = 0 \quad (29)$$

where $P_{(i,j),t}$ is the active branch transmission power from node i to node j at time t , $B_{(i,j)}$ is the branch conductance from node i to node j , $\theta_{i,t}$ and $\theta_{j,t}$ are the voltage phase angles of node i and node j at time t , respectively, $\mathcal{I}^{\text{LINE}}$ is the set of all branches, $\theta_{\text{ref},t} = 0$ is the voltage phase angle of the reference node.

The active power flow transmission constraint of each branch in the electric network is shown in (30).

$$P_{(i,j),\min} \leq P_{(i,j),t} \leq P_{(i,j),\max} \forall (i,j) \in \mathcal{I}^{\text{LINE}}, t \in \mathcal{T} \quad (30)$$

where $P_{(i,j),\min}$ and $P_{(i,j),\max}$ are the minimum and maximum active branch transmission capacity from network node i to node j , $P_{(i,j),\min} = -P_{(i,j),\max}$ denotes that the active branch transmission has a direction.

3) THERMAL NETWORK IMBALANCE CONSTRAINT

Since the heating circulating water has thermal inertia in the thermal network and buildings, the HL is maintained within a limited range to meet the heat demand of customers. The HL imbalance constraint of the thermal network is shown in (31).

$$\begin{aligned} \kappa_{\text{low}} H_t^L &\leq \sum_{b \in \mathcal{I}^{\text{CHP}}} H_{b,t} - \sum_{k \in \mathcal{I}^{\text{HST}}} H_{k,t}^+ + \sum_{k \in \mathcal{I}^{\text{HST}}} H_{k,t}^- \\ &+ \sum_{z \in \mathcal{I}^{\text{Boiler}}} \beta_z P_{z,t} \leq \kappa_{\text{up}} H_t^L \quad \forall t \in \mathcal{T} \end{aligned} \quad (31)$$

where H_t^L is the HL at time t , κ_{low} and κ_{up} are the lower and upper limits of the thermal inertia regulation ratio of the DHN.

IV. CASE STUDIES

The simulations are performed on a computer with an Intel Core i7 CPU and 16 GB of memory. MATLAB-R2020a and the YALMIP toolbox establish the modeling, and the GUROBI optimizer is employed to solve the model of CHP integrating HWPTB.

A. THE SIMULATION STRUCTURE AND DATA OF CHP INTEGRATING HWPTB

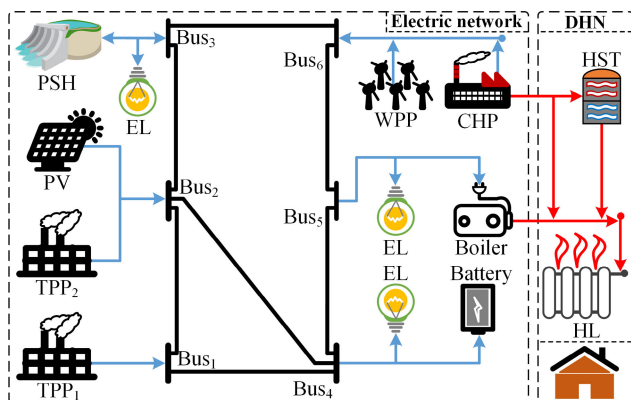


FIGURE 2. The structure diagram of CHP integrating HWPTB.

The structure diagram of CHP integrating HWPTB is shown in Figure 2. The system simulation structure

includes 1 PSH, 1 CHP, 1 PV, 1 WPP, 1 boiler, 1 battery, 1 HST, TPP₁ and TPP₂. The system load ratios of Bus₃-Bus₅ are 40%, 30%, and 30%, respectively, and Bus₁ is the reference node. The detailed simulation data for PSH, CHP, PV, WPP, boiler, battery, HST, and TPPs are shown in Table 2. The simulation data of transmission lines is shown in Table 3. The simulation data for CE is shown in Table 4.

The curves of electric load, heat load, predicted wind and PV power are shown in Figure 3. Due to the positive correlation between EL and human activities and the negative correlation between HL and environmental temperature, the EL peak is opposite to HL. Since the intensity of solar radiation is stronger during the day and weaker at night, wind speeds are stronger at night or early in the morning. Therefore, the predicted PV power is higher during the day, and the predicted wind power is higher at night or early in the morning.

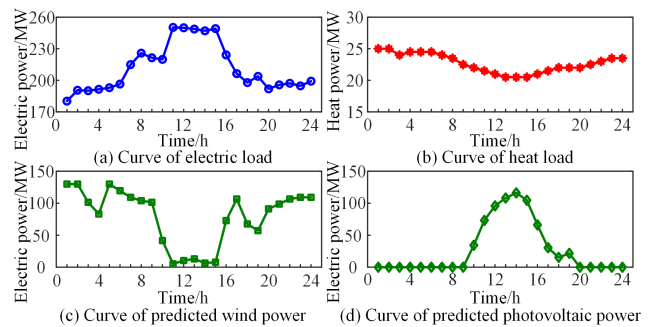


FIGURE 3. Curves of electric load, heat load, predicted wind and PV power.

B. VALIDATION OF CHP INTEGRATING HWPTB

A comparative analysis of four cases is considered to validate the advantage of CHP integrating HWPTB.

- **Case 1:** The traditional optimal scheduling approach combines WPP, PV, CHP, TPPs, batteries and HST. The EL is supplied by WPP, PV, CHP, TPPs, batteries, and the HL is supplied by CHP and HST. The CE, boiler, and PSH operating costs (17)-(19), (20), and (22) are not considered in the objective function (1).

subject to: (3), (4), (6), (8), (9), (11), (13), (15), (16), (28)-(31)

- **Case 2:** To verify the impact of the tiered carbon trading mechanism on the optimal scheduling results, the CE is considered based on Case 1. The boiler and PSH operating costs (20) and (22) are not considered in the objective function (1).

subject to: (3), (4), (6), (8), (9), (11), (13), (15), (16), (28)-(31)

- **Case 3:** To validate the optimal model combining the tiered carbon trading mechanism with boiler for regulating thermal loads and CHP, with the boiler is added to Case 2. The PSH operating cost (22) is not considered in the objective function (1).

TABLE 2. Simulation data of units.

Units	Symbol	Value	Symbol	Value	Symbol	Value	Symbol	Value
PSH[25]	$P_{s,min}^+$	0(MW)	$P_{s,max}^+$	30(MW)	$P_{s,min}^-$	0(MW)	$P_{s,max}^-$	30(MW)
	$E_{s,min}$	0(MWh)	$E_{s,max}$	300(MWh)	$E_{s,ini}$	150(MWh)	$\beta_{s,0}$	0.85
	$\beta_{s,1}$	0.89	$\xi_{s,0}$	82(\$/MW)	$\xi_{s,1}$	45(\$/MW)		
TPP ₁ [26,27]	$P_{f,min}$	10(MW)	$P_{f,max}$	200(MW)	$R_{f,down}$	49.8(MW/h)	$R_{f,up}$	49.8(MW/h)
	$\xi_{f,0}$	0.00049(\$/MW ²)	$\xi_{f,1}$	16.833(\$/MW)	$\xi_{f,2}$	220.576(\$)		
	$\xi_{f,0}$	50(MW)	$P_{f,max}$	200(MW)	$R_{f,down}$	40.2(MW/h)	$R_{f,up}$	40.2(MW/h)
TPP ₂ [26,27]	$P_{f,min}$	10(MW)	$P_{f,max}$	200(MW)	$R_{f,down}$	40.2(MW/h)	$R_{f,up}$	40.2(MW/h)
	$\xi_{f,0}$	0.00125(\$/MW ²)	$\xi_{f,1}$	40.623(\$/MW)	$\xi_{f,2}$	161.868(\$)		
	$\xi_{f,0}$	50(MW)	$P_{f,max}$	200(MW)	$R_{f,down}$	40.2(MW/h)	$R_{f,up}$	40.2(MW/h)
CHP[26,27]	$P_{b,min}$	10(MW)	$P_{b,max}$	200(MW)	$R_{b,down}$	5(MW/h)	$R_{b,up}$	5(MW/h)
	$\xi_{b,0}$	0.00435(\$/MW ²)	$\xi_{b,1}$	3.6(\$/MW)	$\xi_{b,2}$	100(\$)	$H_{b,med}$	38(MW)
	$H_{b,max}$	40(MW)	$v_{b,0}$	-0.16	$v_{b,1}$	1.313	$v_{b,2}$	-0.095
HST[4]	v_b	0.15						
	$H_{k,rated}$	3(MW)	$S_{k,max}$	30(MW)	T_k	20(year)	β_k	0.99
	$\xi_{k,0}$	10(\$/MW)	$\xi_{k,1}$	8000(\$/MW)	$\xi_{k,2}$	4000(\$/MW)		
Battery[4]	$P_{q,rated}$	5(MW)	$S_{q,max}$	55(MW)	T_q	20(year)	β_q	0.95
	$\xi_{q,0}$	26(\$/MW)	$\xi_{q,1}$	15000(\$/MW)	$\xi_{q,2}$	7000(\$/MW)		
	$\xi_{z,t}(Peak)$	77(\$/MW)	$\xi_{z,t}(Valley)$	46(\$/MW)	$P_{z,max}$	5(MW)	β_z	0.98
Boiler[4]	$\xi_{g,0}$	171.227(\$/MW)						
WPP[26,27]	$\xi_{r,0}$	140(\$/MW)						
PV[4]								

TABLE 3. Simulation data of transmission lines [28].

Line NO	From Bus	To Bus	B (pu)	Flow limit(MW)
1	1	2	0.17	200
2	1	4	0.258	130
3	2	3	0.197	130
4	2	4	0.018	130
5	3	6	0.037	130
6	4	5	0.037	130
7	5	6	0.14	130

TABLE 4. Simulation data of CE [29].

Symbol	Value	Symbol	Value	Symbol	Value
ϵ_f	0.877	ϵ_b	0.979	ϵ_g	1.1
ϵ_r	1.1	β_f	0.94	β_b	1.03
ω	6.9(\$/MW)	\varkappa	100	φ	0.25

subject to: (3), (4), (6), (8), (9), (11), (13), (15), (16), (21), (28)- (31)

- **Case 4:** To verify the advantage of PSH in CHP integrating HWPTB and to compare it with previous cases, PSH is added to Case 3.

subject to: (3), (4), (6), (8), (9), (11), (13), (15), (16), (21), (23)- (31)

The method proposed in this paper is verified through four cases. Case 1 serves as the baseline, representing the traditional optimal method of CHP. Case 2 considers tiered carbon trading based on Case 1, aiming to verify the impact of carbon trading on the system. Boilers convert electric energy into heat energy and are commonly used in CHP scheduling, similar to the role of PSH. To highlight the advantages of PSH in the CEHS, Case 3 incorporates boilers. Based on the above three cases, the integration of PSH and CHP is analyzed in Case 4 to determine the effect of PSH on optimal

scheduling results, specifically whether the addition of PSH has a positive or negative impact.

1) COMPARISON OF SCHEDULING RESULTS OF ELECTRIC POWER

The electric power scheduling results for four cases are shown in Figure 4, Tables 5, 6, 7, and 8. In the tables, the negative and positive values for batteries represent charging and discharging, respectively, while the negative and positive values for PSH represent water pumping and power generation, respectively. Comparing Case 4 with Case 3, due to the lower operating costs of PSH compared to TPP₁, TPP₁ operates at the minimum output of the unit. The number of battery charging and discharging cycles and the frequency of boiler usage are significantly reduced. Additionally, Case 4 increases the accommodation of wind power at 1:00, 2:00, 5:00, 6:00, and 23:00, as well as the accommodation of PV at 14:00, 16:00, and 17:00. During periods of high wind power output, such as 1:00, 2:00, 5:00, and 21:00-24:00, PSH operates at maximum power to store water using wind power, while CHP operates at minimum power. When the wind power output is reduced, due to the low operating cost of PSH and the high operating cost of TPPs, the adjustment flexibility of CHP increases. While absorbing photovoltaic output, the goal is to minimize the total operating cost by reducing the operating cost of HST heat storage and release, and increasing its electric power output. Compared to Case 2, Case 3 considers the use of a boiler. Therefore, the boiler operates during periods of high wind power output, such as 1:00-3:00, 5:00, 6:00, 16:00, 17:00, and 22:00-24:00, to minimize WPC. Compared to Case 1, tiered carbon trading is considered in Case 2, where the power output from conventional units and CHP is reduced and the power consumed by wind and PV power is increased.

The electric power scheduling results of TPPs for four cases are shown in Figure 5. Since CE, boiler, and PSH are considered in Case 2, Case 3, and Case 4, respectively, the

TABLE 5. The electric power scheduling results of case 1.

Units	1	2	3	4	5	6	7	8	9	10	11	12	13	14	15	16	17	18	19	20	21	22	23	24/h
EL/MW	180.3	190.6	190.2	191.5	193	196.5	215	225.9	221.5	220	250.3	250	248.8	247.1	249.2	224.2	206.4	197.9	203.8	191.9	195.7	197.2	194.8	199.2
Battery/MW	-5	-5	-5	2.2	-4.1	-4.4	0.03	5	4.3	5	5	5	5	5	5	-5	-5	5	5	0	-3.1	-5	-5	-5
WPP/MW	85.9	94	94.1	83.2	96	100.1	109.2	104	101.4	41.6	5.2	10.4	13	6.5	7.8	72.8	106.6	67.6	57.2	91.3	98.8	103.3	100.9	105.3
PV/MW	0	0	0	0	0	0	0	0	0	34.3	73.2	94	104	106	104.4	58.3	6.8	15.4	21.7	0	0	0	0	0
CHP/MW	39.4	41.6	41.1	46.1	41.1	40.7	45.7	50.7	55.7	60.7	63.1	58.1	53.1	48.1	43.1	38.1	38	43	45.6	40.6	40	38.9	38.9	38.9
TPP ₂ /MW	50	50	50	50	50	50	50	50	50	50	50	50	50	50	50	50	50	50	50	50	50	50	50	50
TPP ₁ /MW	10	10	10	10	10	10	10	16.1	10	28.3	53.9	32.5	23.7	31.6	38.9	10	10	16.9	24.3	10	10	10	10	10

TABLE 6. The electric power scheduling results of case 2.

Units	1	2	3	4	5	6	7	8	9	10	11	12	13	14	15	16	17	18	19	20	21	22	23	24/h
EL/MW	180.3	190.6	190.2	191.5	193	196.5	215	225.9	221.5	220	250.3	250	248.8	247.1	249.2	224.2	206.4	197.9	203.8	191.9	195.7	197.2	194.8	199.2
Battery/MW	-5	-5	-5	2.5	-5	-5	0	5	3.6	5	5	5	5	5	5	-5	-5	5	5	0	-1.1	-5	-5	-5
WPP/MW	85.9	96.3	97.1	83.2	99.3	102.7	109.2	104	101.4	41.6	5.2	10.4	13	6.5	7.8	72.8	106.6	67.6	57.2	91.3	98.8	104.2	101.8	106.2
PV/MW	0	0	0	0	0	0	0	0	0	34.3	73.2	95.9	108.2	110.1	104.7	53.4	6.8	15.4	21.7	0	0	0	0	0
CHP/MW	39.4	39.4	38.1	43.1	38.7	38.7	43.7	48.7	53.7	58.7	63.7	63	58	53	48	43	38	43	45.6	40.6	38	38	38	38
TPP ₂ /MW	50	50	50	50	50	50	50	50	50	50	50	50	50	50	50	50	50	50	50	50	50	50	50	50
TPP ₁ /MW	10	10	10	12.8	10	10	12.1	18.1	12.8	30.4	53.3	25.7	14.6	22.5	33.7	10	10	16.9	24.3	10	10	10	10	10

TABLE 7. The electric power scheduling results of case 3.

Units	1	2	3	4	5	6	7	8	9	10	11	12	13	14	15	16	17	18	19	20	21	22	23	24/h
EL/MW	180.3	190.6	190.2	191.5	193	196.5	215	225.9	221.5	220	250.3	250	248.8	247.1	249.2	224.2	206.4	197.9	203.8	191.9	195.7	197.2	194.8	199.2
Battery/MW	-5	-5	-5	2.2	-5	-5	0	5	3.9	5	5	5	5	5	5	-5	-5	5	5	0	-1.1	-5	-5	-5
Boiler/MW	5	5	4.3	0	5	5	0	0	0	0	0	0	0	0	0	0	5	5	0	0	0	2.4	5	3
WPP/MW	92.3	102.6	101.4	83.2	105	108.4	109.2	104	101.4	41.6	5.2	10.4	13	6.5	7.8	72.8	106.6	67.6	57.2	91.3	98.8	106.6	106.7	109.2
PV/MW	0	0	0	0	0	0	0	0	0	34.3	73.2	95.9	108.2	110.3	104.7	58	11.4	15.4	21.7	0	0	0	0	0
CHP/MW	38	38	38.1	43.1	38.1	38.1	43.1	48.1	53.1	58.1	63.1	63.4	58.4	53.4	48.4	43.4	38.4	43.4	45.6	40.6	38	38	38	38
TPP ₂ /MW	50	50	50	50	50	50	50	50	50	50	50	50	50	50	50	50	50	50	50	50	50	50	50	50
TPP ₁ /MW	10	10	10	13.1	10	10	12.7	18.8	13.1	31	53.9	25.3	14.2	22	33.4	10	10	16.6	24.3	10	10	10	10	10

TABLE 8. The electric power scheduling results of case 4.

Units	1	2	3	4	5	6	7	8	9	10	11	12	13	14	15	16	17	18	19	20	21	22	23	24/h
EL/MW	180.3	190.6	190.2	191.5	193	196.5	215	225.9	221.5	220	250.3	250	248.8	247.1	249.2	224.2	206.4	197.9	203.8	191.9	195.7	197.2	194.8	199.2
PSH/MW	-30	-30	-9.2	5.3	-30	-24.1	-0.2	8.1	4.1	23.1	30	17.6	3.9	3.5	23	-23.5	-30	6.2	19.3	0	-1.1	-7.4	-12.4	-8
Battery/MW	-5	-2.6	0	0	-0.8	0	0	2.8	0	0	5	0	0	5	0	0	-4.4	0	0	0	0	0	0	0
Boiler/MW	5	4.8	0.05	0	4.2	0	0	0	0	0	0	0	0	0	0	0	0	0	0	0	0	0	0	0
WPP/MW	122.3	130	101.4	83.2	130	119.6	109.2	104	101.4	41.6	5.2	10.4	13	6.5	7.8	72.8	106.6	67.6	57.2	91.3	98.8	106.6	109.2	109.2
PV/MW	0	0	0	0	0	0	0	0	0	34.3	73.2	95.9	108.2	113.3	104.7	66.2	30.5	15.4	21.7	0	0	0	0	0
CHP/MW	38	38	38	43	38	41	46	51	56	60.9	66	66	63.7	58.7	53.7	48.7	43.7	48.7	45.6	40.6	38	38	38	38
TPP ₂ /MW	50	50	50	50	50	50	50	50	50	50	50	50	50	50	50	50	50	50	50	50	50	50	50	50
TPP ₁ /MW	10	10	10	10	10	10	10	10	10	10	21	10	10	10	10	10	10	10	10	10	10	10	10	10

electric power output from TPPs gradually decreases during the period from 11:00-15:00. Especially during the period of 12:00-15:00, the TPP outputs at the minimum operating power. The trend of the curves of the TPPs can be verified by the sum of conventional unit costs.

The electric power scheduling results of CHP for four cases are shown in Figure 6. Since wind power output is higher from 1:00-10:00 and 21:00-24:00, the output of traditional units is reduced to absorb wind power in Case 1. However, due to HL demand, the wind power accommodation is limited. Therefore, the output power of CHP is higher than that of the other three cases.

The electric power scheduling result of PSH in Case 4 is shown in Figure 7. PSH, WPP, and PV energy are renewable energy. However, due to PSH using water as an energy storage medium for storing and regulating electric energy, the difference is that PSH can be controlled. During valley periods of the grid, typically from 1:00-6:00 and 21:00-24:00, the excess electric energy is used to pump water from the downstream reservoir to the upstream reservoir, and the wind power is converted to gravitational potential energy stored in the water. During the peak times of 7:00-20:00, water is released to generate electricity, converting the stored gravitational potential energy back into electrical energy

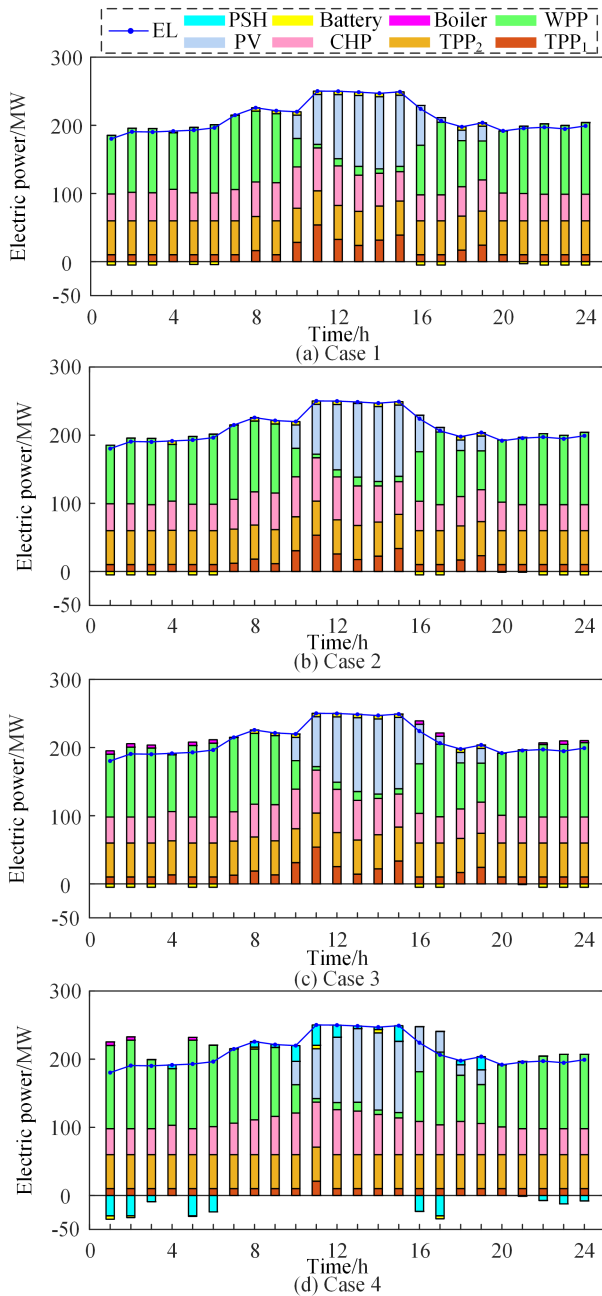


FIGURE 4. The electric power scheduling results for four cases.

to meet the demand for power during peak load periods. Moreover, due to the penalty associated with discarding renewable energy, PSH generates electricity at 4:00, 18:00, and 19:00 when wind power output decreases. Therefore, the PSH generates electricity to supply the electric load demand at 4:00, 18:00 and 19:00. When the wind power output decreases, the output of conventional thermal generation and CHP is reduced, the flexibility of CHP is improved, and the CE is reduced.

The electric power scheduling results of the battery for four cases are shown in Figure 8. Compared to Case 1,

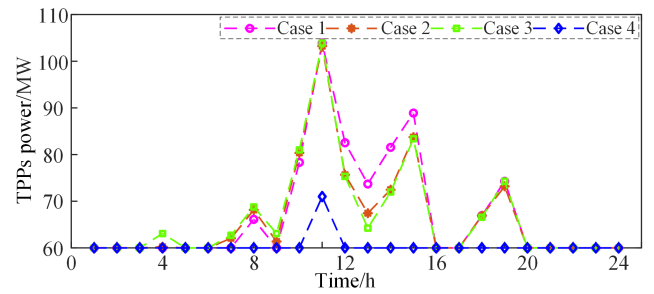


FIGURE 5. The electric power scheduling results of TPPs for four cases.

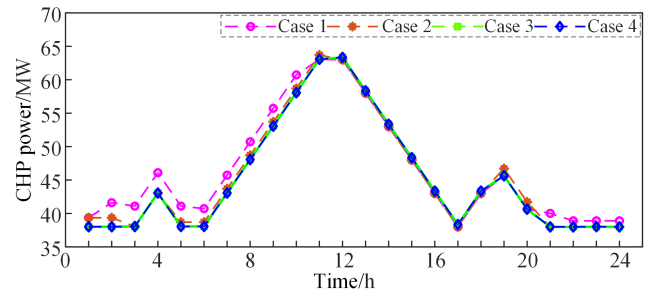


FIGURE 6. The electric power scheduling results of CHP for four cases.

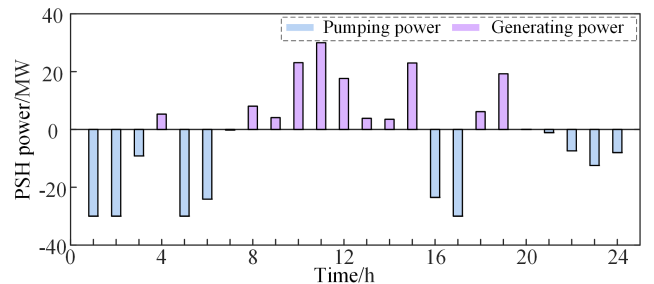


FIGURE 7. The electric power scheduling result of PSH in case 4.

tiered carbon trading is considered in Case 2. When wind power increases or decreases at 4:00, 5:00, and 6:00, the battery charges and discharges with the maximum power. However, the PV power output is increased at 13:00, and the discharging power of the battery is reduced to increase the accommodation of PV. Due to the increased boiler in Case 3, there is still 4.74% of WPC and 4.96% of PVPC. Therefore, the charging and discharging power of the battery in Case 3 are consistent with the trend in Cases 1 and 2. Since the PSH is utilized in Case 4, there is no need to reduce the output of traditional thermal generation and CHP to accommodate wind and PV power. Therefore, the charging power of the battery in Case 4 is reduced compared to the other three cases.

2) COMPARISON OF SCHEDULING RESULTS OF THERMAL POWER

The thermal power scheduling results for four cases are shown in Figure 9. Compared with Case 1, since tiered carbon

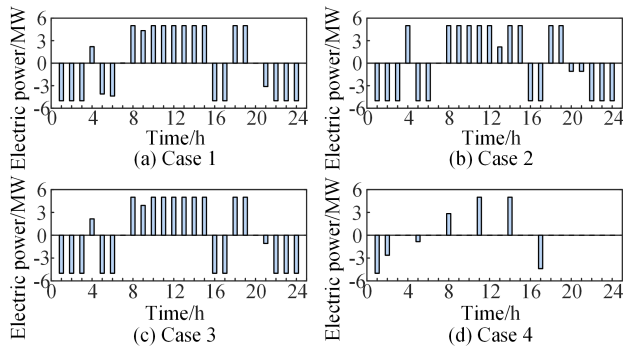


FIGURE 8. The electric power scheduling results of the battery for four cases.

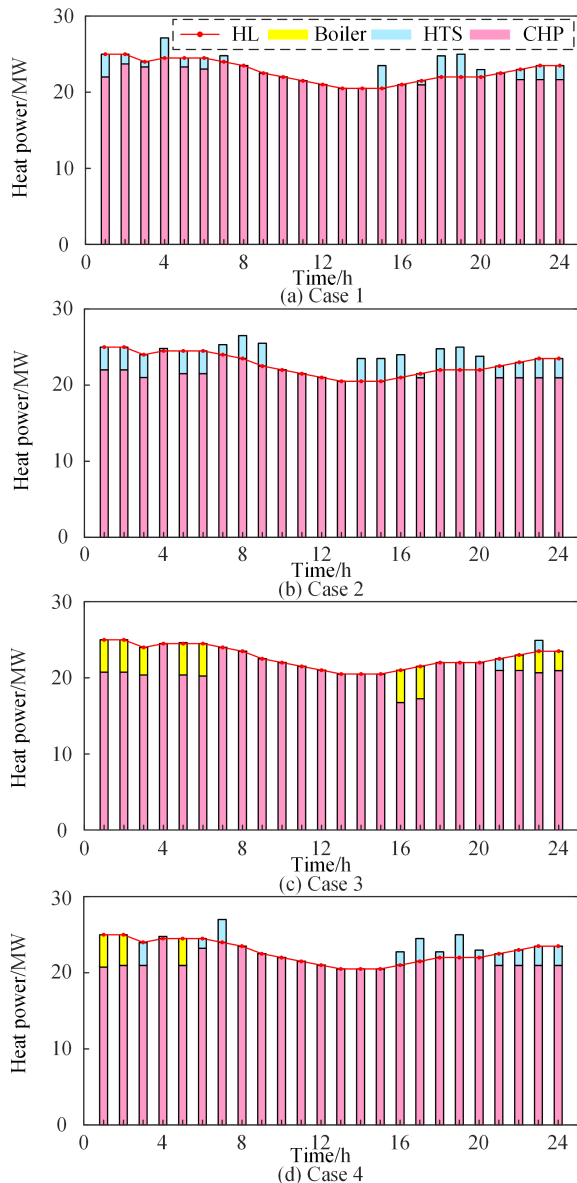


FIGURE 9. The thermal power scheduling results for four cases.

trading is considered in Case 2, when wind power output increases at 1:00-6:00 and 21:00-24:00, HTS releases the

thermal energy during this period, reducing the CHP output power. Significantly, when the wind power output decreases at 4:00, the HL demand is only met by CHP in Case 2. However, the CHP output power in Case 1 is greater than the EL, and the excess heat is stored by HTS. Therefore, the thermal energy storage and release of HTS in Case 2 are more flexible, and the CHP output and CE are reduced. Due to the addition of the boiler in Case 3, electrical energy is used by the boiler to generate thermal energy, which not only increases the accommodation of renewable energy, but also releases the generated thermal energy. Therefore, to improve the flexibility of CHP, the boiler is utilized to consume electric power to reduce the CHP output. Compared to Case 3, the thermal energy released by the boiler is reduced in Case 4. Since the operating cost of the boiler is higher than that of the PSH, the boiler is only utilized between 1:00-2:00 and 5:00 when the wind power output is high, and the PSH is limited by their operating power. The boiler continues to consume electric power that cannot be accommodated. However, during other periods, to reduce system operating costs, the PSH is utilized to consume electric power, and the HTS is used to store thermal energy.

The thermal power scheduling results of HTS for four cases are shown in Figure 10. The change of the thermal energy storage and release power of HTS in Figure 10 are consistent with those in Figure 9. Due to tiered carbon trading, boiler and PSH are considered in Cases 2, 3, and 4. Therefore, the thermal energy storage and release power of HTS increase in Case 2, the thermal energy release of the boiler reduces the thermal energy storage and release of HTS in Case 3, and the combination of boiler and PSH not only reduces the thermal energy storage and release power of HTS but also reduces operating costs in Case 4.

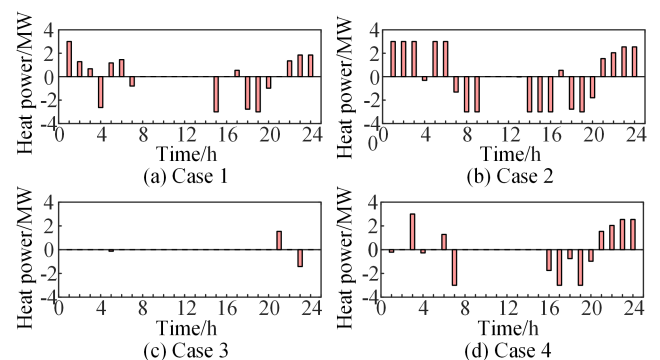


FIGURE 10. The thermal power scheduling results of HTS for four cases.

3) COMPARISON OF OPERATION COSTS, WPC, AND PVPC

The numerical simulation results, WPC, and PVPC for four cases are presented in Table 9. Compared with the traditional optimal dispatch method in Case 1, tiered carbon trading is added in Case 2. Thus, the operating costs of traditional thermal power and CHP units are reduced by 0.18%. The WPC and PVPC rates are reduced by 0.76% and 0.82%,

respectively. The corresponding costs of WPC and PVPC are reduced by 2,391 (\$) and 760.6 (\$). Since the CE in Case 2 is larger than the quota, the CE cost of 244.7 (\$) is increased. However, the total operating cost of the system is reduced by 3045 (\$). Case 2 increases the CE cost compared to Case 1, the operating cost of CHP in the system is reduced. Due to the boiler being added in Case 3, the operating cost of the boiler is increased compared to Case 2, however, tiered carbon trading profits 413.4 (\$). Compared with Case 1, the WPC and PVPC rates are further decreased by 2.65% and 2.24%, respectively, and the operating cost of the system and CHP are reduced accordingly. The PSH is added in Case 4, in which the operating cost is 6999.5 (\$), and tiered carbon trading further profits 4163.3 (\$). The WPC and PVPC are almost non-existent compared to Case 1, and the system and CHP operating costs are the lowest of the four cases. The order of WPC, PV curtailment, operation costs of traditional units, and total costs for the four cases are as follow: Case 1 > Case 2 > Case 3 > Case 4. Therefore, compared to the conventional method, the economy of the system operation is improved in this paper.

TABLE 9. Numerical simulation results, WPC, and PVPC for four cases.

Costs and power curtailment	Case1	Case2	Case3	Case4
Total cost (\$)	108,374	105,329	98,647	75,491
Conventional units cost (\$)	74,909.6	74,772.3	74,308.3	70,291.6
WPC cost (\$)	26,755	24,364	17,762	1320.1
WPC rate (%)	7.39	6.63	4.74	0.22
PVPC cost (\$)	6,709.4	5,948.8	4,626.5	400.5
PVPC rate (%)	7.2	6.38	4.96	0.43
CE cost (\$)	×	244.7	-413.4	-4,163.3
Boiler cost (\$)	×	×	2,364.2	642.4
PSH cost (\$)	×	×	×	6,999.5

The curves of predicted and scheduled wind power for four cases are shown in Figure 11. During 1:00-3:00, 5:00-6:00, and 22:00-24:00, WPC occurs in Case 1-Case 3, and the wind power changes during these time periods are consistent with the WPC rates shown in Table 9. In Case 4, there is no WPC during the periods of 2:00-3:00, 5:00-6:00, and 22:00-24:00. With the deployment of a larger-capacity boiler or PSH, the WPC can be fully absorbed.

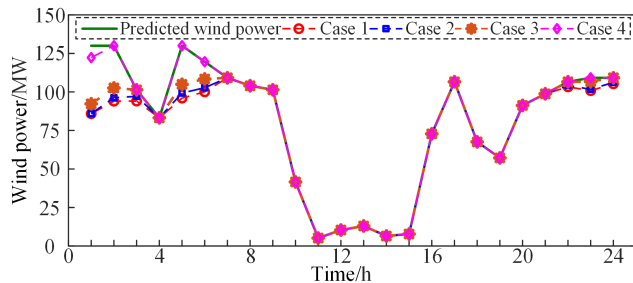


FIGURE 11. The curves of predicted and scheduled wind power for four cases.

The curves of predicted and scheduled PV for four cases are shown in Figure 12. Due to the larger PV output power

during the 12:00-14:00 time period and the constraints of the EL and HL, the PV power consumed by the tiered carbon trading, boiler, and PSH cases is larger than that of Case 1, with Case 4 absorbing the maximum PV power. Since the wind power increases at 17:00 and the penalty for WPC is greater than that for PVPC, there is still PVPC in Case 1-Case 3, while the PV output power of Case 4 can be utilized by the PSH, and there is no PVPC in Case 4 at 16:00 and 17:00.

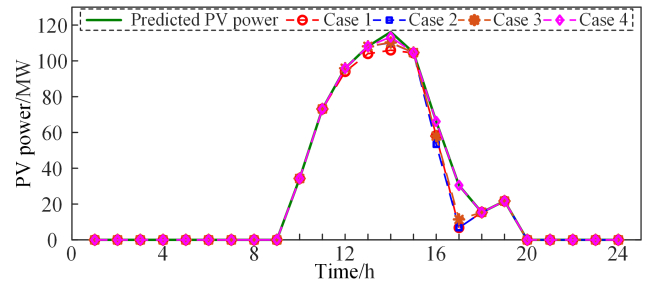


FIGURE 12. The curves of predicted and scheduled PV power for four cases.

4) COMPARISON OF CE COSTS IN THREE CASES

The CE costs from Case 2 to Case 4 are shown in Table 10. The first row of the Table 10, from 1 to 24, indicates the scheduling period T . To distinguish between the profit and cost of utilizing the tiered carbon trading mechanism, the highlighted colour numbers in Table 10 represent negative values, i.e., the profits obtained through the tiered carbon trading mechanism. In contrast, the non-highlighted colour numbers represent positive values. The physical meaning of positive and negative values is explained in Section III-B7. The three different highlighted colours are used to distinguish the three cases. The tiered carbon trading costs displayed in the Table 10 are rounded. The tiered carbon trading costs at various scheduling periods are presented. Compared with the other two cases, Case 4 not only does not increase CE costs at 8:00, 9:00, 12:00, and 15:00, but also generates profits during these periods, and the profits obtained are greater than those in the other two cases. Moreover, at 4:00, 10:00, 11:00, and 18:00-20:00, the CE costs are also less than or equal to those in the other two cases. Similarly, the CE costs in Case 3 are superior to those in Case 2.

Table 10 shows the numerical quantification results of the tiered carbon trading costs. To facilitate readers' understanding, Figure 13 presents the curves of the CE costs. It can be observed that the curve of the three cases remains consistent. However, due to differences in scheduling resources and system flexibility among the cases, the curves for Cases 2 and 3 are significantly higher than those for Case 4. As mentioned above, lower curves indicate negative profits, indicating greater system profits. Compared to Case 2, Case 3 exhibits significantly higher profits during 1:00-3:00, 5:00, 6:00, 16:00, 17:00, and 21-24:00.

The above results indicate that the addition of PSH units reduces the CE and the highest profits. This is because

TABLE 10. The CE costs from case 2 to case 4.

Case	1	2	3	4	5	6	7	8	9	10	11	12	13	14	15	16	17	18	19	20	21	22	23	24
2(\$)	87	50	70	191	94	140	159	40	20	621	931	80	346	194	18	501	295	237	418	25	92	163	131	190
3(\$)	5	142	126	196	173	218	153	46	21	627	938	76	349	202	15	567	361	234	418	25	92	195	196	229
4(\$)	402	504	126	146	504	347	178	77	10	307	426	153	383	406	327	652	605	163	188	25	92	195	229	229

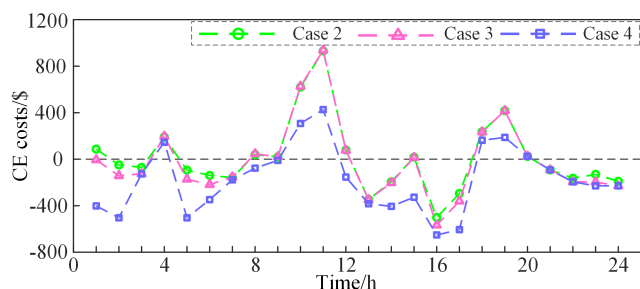


FIGURE 13. The curves of CE costs from case 2 to case 4.

the Northwest region of China is rich in water resources, which can effectively assist the combined heat and power system in achieving bidirectional development of heating and renewable energy accommodation. Concerning renewable energy base in a region of Northwest China, it is verified that PSH can effectively regulate the fluctuations of wind and photovoltaic power output in the combined heat and power system, improving the stability and low-carbon benefits of the system. This fully demonstrates that energy storage can effectively coordinate the complementarity of multiple energy sources.

V. CONCLUSION

To meet the heat demand of users in the CHP system and enhance the accommodation of renewable energy. A low-carbon optimal scheduling method that integrates HWPTB with CHP is proposed, and the scheduling model for coordinated multi-energy complementarity of HWPTB is developed. The results show that renewable energy accommodation, reduction of CE, and economy of system operation are enhanced.

Four cases are compared, and a 6-bus system is used to verify the proposed method. The following conclusions are obtained: the WPC rates are 7.39%, 6.63%, 4.74%, and 0.22%, respectively, and the PVPC rates are 7.2%, 6.38%, 4.96%, and 0.43%, respectively. The rates of WPC and PVPC are gradually decreasing, and compared with the traditional optimal scheduling method without considering carbon trading and PSH, the accommodation of wind and PV is improved by 7.17% and 6.77% in the integrated PSH with CHP systems, respectively. The CE costs for the three cases considering tiered carbon trading are 244.7 (\$), -413.4 (\$), and -4163.3 (\$), respectively. It can be observed that the HWPTB system that considers PSH not only avoids increasing the CE cost but also generates 4163.3 (\$) profit through carbon trading. The total operation cost of the HWPTB system is 75,491 (\$), which is reduced by 43.6%

compared to the case without PSH and carbon trading, and the economy of the system is enhanced. The results of this work can promote the development of a clean energy base integrating hydropower, wind, PV, and energy storage in Northwest China.

ACKNOWLEDGMENT

This work was also supported by Research and Engineering Demonstration of a Fully Clean Energy Safe, Autonomous, and Controllable Smart Management and Control System at the 10-GW Level (Grant No. CSIEKJ220700539).

REFERENCES

- [1] H. Hua, X. Chen, L. Gan, J. Sun, N. Dong, D. Liu, Z. Qin, K. Li, and S. Hu, "Demand-side joint electricity and carbon trading mechanism," *IEEE Trans. Ind. Cyber-Phys. Syst.*, vol. 2, pp. 14–25, Nov. 2024, doi: 10.1109/TICPS.2023.3335328.
- [2] W. Lian, X. Sun, Y. Wang, H. Duan, T. Gao, and Q. Yan, "The mechanism of China's renewable energy utilization impact on carbon emission intensity: Evidence from the perspective of intermediary transmission," *J. Environ. Manage.*, vol. 350, Jan. 2024, Art. no. 119652, doi: 10.1016/j.jenvman.2023.119652.
- [3] J. Luo, W. Zhuo, S. Liu, and B. Xu, "The optimization of carbon emission prediction in low carbon energy economy under big data," *IEEE Access*, vol. 12, pp. 14690–14702, 2024, doi: 10.1109/ACCESS.2024.3351468.
- [4] H. Ji, H. Wang, J. Yang, J. Feng, Y. Yang, and M. O. Okoye, "Optimal schedule of solid electric thermal storage considering consumer behavior characteristics in combined electricity and heat networks," *Energy*, vol. 234, Nov. 2021, Art. no. 121237, doi: 10.1016/j.energy.2021.121237.
- [5] Y. Song and L. Shi, "Dynamic economic dispatch with CHP and wind power considering different time scales," *IEEE Trans. Ind. Appl.*, vol. 58, no. 5, pp. 5734–5746, Sep. 2022, doi: 10.1109/TIA.2022.3188603.
- [6] G. Moustafa, H. Alnami, S. H. Hakmi, A. M. Shaheen, A. R. Ginidi, M. A. Elshahed, and H. S. E. Mansour, "A novel mantis search algorithm for economic dispatch in combined heat and power systems," *IEEE Access*, vol. 12, pp. 2674–2689, 2024, doi: 10.1109/ACCESS.2023.3344679.
- [7] A. M. Shaheen, R. A. El-Sehiemy, E. Elattar, and A. R. Ginidi, "An amalgamated heap and jellyfish optimizer for economic dispatch in combined heat and power systems including N-1 unit outages," *Energy*, vol. 246, May 2022, Art. no. 123351, doi: 10.1016/j.energy.2022.123351.
- [8] X. Chen, C. Kang, M. O'Malley, Q. Xia, J. Bai, C. Liu, R. Sun, W. Wang, and H. Li, "Increasing the flexibility of combined heat and power for wind power integration in China: Modeling and implications," *IEEE Trans. Power Syst.*, vol. 30, no. 4, pp. 1848–1857, Jul. 2015, doi: 10.1109/TPWRS.2014.2356723.
- [9] Y. Du, Y. Xue, W. Wu, M. Shahidehpour, X. Shen, B. Wang, and H. Sun, "Coordinated planning of integrated electric and heating system considering the optimal reconfiguration of district heating network," *IEEE Trans. Power Syst.*, vol. 39, no. 1, pp. 794–808, Jan. 2024, doi: 10.1109/TPWRS.2023.3242652.
- [10] C. Lin, W. Wu, B. Wang, M. Shahidehpour, and B. Zhang, "Joint commitment of generation units and heat exchange stations for combined heat and power systems," *IEEE Trans. Sustain. Energy*, vol. 11, no. 3, pp. 1118–1127, Jul. 2020, doi: 10.1109/TSTE.2019.2917603.
- [11] B. Liu, J. Li, S. Zhang, M. Gao, H. Ma, G. Li, and C. Gu, "Economic dispatch of combined heat and power energy systems using electric boiler to accommodate wind power," *IEEE Access*, vol. 8, pp. 41288–41297, 2020, doi: 10.1109/ACCESS.2020.2968583.

- [12] M. R. Elkadeem and M. A. Abido, "Optimal planning and operation of grid-connected PV/CHP/battery energy system considering demand response and electric vehicles for a multi-residential complex building," *J. Energy Storage*, vol. 72, Nov. 2023, Art. no. 108198, doi: [10.1016/j.est.2023.108198](https://doi.org/10.1016/j.est.2023.108198).
- [13] M. Sarlak, A. Samimi, M. Nikzad, and A. H. Salemi, "IGDT-based robust operation of thermal and electricity energy-based microgrid with distributed sources, storages, and responsive loads," *Int. Trans. Electr. Energy Syst.*, vol. 2022, pp. 1–20, Dec. 2022, doi: [10.1155/2022/6002695](https://doi.org/10.1155/2022/6002695).
- [14] L. Shi, M.-W. Tian, A. Alizadeh, A. Mohammadzadeh, and S. Nojavan, "Information gap decision theory-based risk-averse scheduling of a combined heat and power hybrid energy system," *Sustainability*, vol. 15, no. 6, p. 4825, Mar. 2023, doi: [10.3390/su15064825](https://doi.org/10.3390/su15064825).
- [15] N. Naval, J. M. Yusta, R. Sánchez, and F. Sebastián, "Optimal scheduling and management of pumped hydro storage integrated with grid-connected renewable power plants," *J. Energy Storage*, vol. 73, Dec. 2023, Art. no. 108993, doi: [10.1016/j.est.2023.108993](https://doi.org/10.1016/j.est.2023.108993).
- [16] S. Guo, A. Kurban, Y. He, F. Wu, H. Pei, and G. Song, "Multi-objective sizing of solar-wind-hydro hybrid power system with doubled energy storages under optimal coordinated operational strategy," *CSEE J. Power Energy Syst.*, vol. 9, no. 6, pp. 2144–2155, Nov. 2023, doi: [10.17775/CSEEJPES.2021.00190](https://doi.org/10.17775/CSEEJPES.2021.00190).
- [17] Y. Ren, K. Jin, C. Gong, J. Hu, D. Liu, X. Jing, and K. Zhang, "Modelling and capacity allocation optimization of a combined pumped storage/wind/photovoltaic/hydrogen production system based on the consumption of surplus wind and photovoltaics and reduction of hydrogen production cost," *Energy Convers. Manage.*, vol. 296, Nov. 2023, Art. no. 117662, doi: [10.1016/j.enconman.2023.117662](https://doi.org/10.1016/j.enconman.2023.117662).
- [18] X. Li, Z. Tan, J. Shen, J. Yang, W. Fan, H. Zhao, and T. Zhang, "Research on the operation strategy of joint wind-photovoltaic-hydropower-pumped storage participation in electricity market based on Nash negotiation," *J. Cleaner Prod.*, vol. 442, Feb. 2024, Art. no. 140981, doi: [10.1016/j.jclepro.2024.140981](https://doi.org/10.1016/j.jclepro.2024.140981).
- [19] I. Amoussou, E. Tanyi, A. Ali, T. F. Agajie, B. Khan, J. B. Ballester, and W. B. Nsanyu, "Optimal modeling and feasibility analysis of grid-interfaced solar PV/wind/pumped hydro energy storage based hybrid system," *Sustainability*, vol. 15, no. 2, p. 1222, Jan. 2023, doi: [10.3390/su15021222](https://doi.org/10.3390/su15021222).
- [20] X. Guo and X. Yang, "The development of wind power under the low-carbon constraints of thermal power in the Beijing-Tianjin-Hebei region," *IEEE Access*, vol. 8, pp. 44783–44797, 2020, doi: [10.1109/ACCESS.2020.2978282](https://doi.org/10.1109/ACCESS.2020.2978282).
- [21] D. Zou, D. Gong, and H. Ouyang, "The dynamic economic emission dispatch of the combined heat and power system integrated with a wind farm and a photovoltaic plant," *Appl. Energy*, vol. 351, Dec. 2023, Art. no. 121890, doi: [10.1016/j.apenergy.2023.121890](https://doi.org/10.1016/j.apenergy.2023.121890).
- [22] Q. Wang, J. Guo, and R. Li, "Better renewable with economic growth without carbon growth: A comparative study of impact of turbine, photovoltaics, and hydropower on economy and carbon emission," *J. Cleaner Prod.*, vol. 426, Nov. 2023, Art. no. 139046, doi: [10.1016/j.jclepro.2023.139046](https://doi.org/10.1016/j.jclepro.2023.139046).
- [23] Y. Xiang, M. Fang, J. Liu, P. Zeng, P. Xue, and G. Wu, "Distributed dispatch of multiple energy systems considering carbon trading," *CSEE J. Power Energy Syst.*, vol. 9, no. 2, pp. 459–469, Mar. 2023, doi: [10.17775/CSEEJPES.2021.09050](https://doi.org/10.17775/CSEEJPES.2021.09050).
- [24] Y. Cao, C. Zhao, and D. Li, "Carbon management for intelligent community with combined heat and power systems," *Sustainability*, vol. 15, no. 17, p. 13257, Sep. 2023, doi: [10.3390/su151713257](https://doi.org/10.3390/su151713257).
- [25] M. A. Nasab, M. Zand, S. Padmanaban, M. S. Bhaskar, and J. M. Guerrero, "An efficient, robust optimization model for the unit commitment considering renewable uncertainty and pumped-storage hydropower," *Comput. Electr. Eng.*, vol. 100, May 2022, Art. no. 107846, doi: [10.1016/j.compeleceng.2022.107846](https://doi.org/10.1016/j.compeleceng.2022.107846).
- [26] Z. Li, W. Wu, J. Wang, B. Zhang, and T. Zheng, "Transmission-constrained unit commitment considering combined electricity and district heating networks," *IEEE Trans. Sustain. Energy*, vol. 7, no. 2, pp. 480–492, Apr. 2016, doi: [10.1109/TSTE.2015.2500571](https://doi.org/10.1109/TSTE.2015.2500571).
- [27] Y. Fang, S. Zhao, N. Wang, Z. Li, and J. Liu, "Power system stochastic optimal dispatch considering thermal and electrical coordination," *Int. J. Electr. Power Energy Syst.*, vol. 110, pp. 772–780, Sep. 2019, doi: [10.1016/j.ijepes.2019.03.065](https://doi.org/10.1016/j.ijepes.2019.03.065).
- [28] Y. Dai, L. Chen, Y. Min, Q. Chen, J. Hao, K. Hu, and F. Xu, "Dispatch model for CHP with pipeline and building thermal energy storage considering heat transfer process," *IEEE Trans. Sustain. Energy*, vol. 10, no. 1, pp. 192–203, Jan. 2019, doi: [10.1109/TSTE.2018.2829536](https://doi.org/10.1109/TSTE.2018.2829536).
- [29] G. Lv, Y. Zhang, J. Zhu, L. Liu, Y. Wu, and T. Wang, "Low-carbon optimal operation of electricity-heat-gas systems based on bi-directional tiered-pricing carbon trading," *Energy Rep.*, vol. 9, pp. 377–387, Sep. 2023, doi: [10.1016/j.egyr.2023.04.116](https://doi.org/10.1016/j.egyr.2023.04.116).



SHENGANG ZHU was born in Huangyuan County, Qinghai, China, in September 1972. He received the master's degree. He is currently a Senior Economist. His research interest includes new energy economy.



ENZHONG WANG was born in Leshan, Sichuan, China, in September 1982. He received the bachelor's degree. He is currently a Senior Engineer. His research interests include hydropower and new energy.



SHAOZU HAN was born in Datou, Shanxi, China, in April 1992. He received the master's degree. He is currently a Engineer. His research interests include automation and new electric power systems.



HUICHAO JI received the B.S. degree in measurement and control technology and instruments from Jilin Institute of Chemical Technology, Jilin, China, in 2010, the M.S. degree in control engineering from Northeast Electric Power University, Jilin, in 2015, and the Ph.D. degree in electrical engineering from Shenyang University of Technology, Shenyang, China, in 2022. He is currently a Lecturer with Northeast Electric Power University. His research interests include smart grids, power system optimization, and electric and thermal energy storage technology.

...